RESEARCH ARTICLE SUMMARY

PLANETARY SCIENCE

Detection of local H_2O exposed at the surface of Ceres

Jean-Philippe Combe,* Thomas B. McCord, Federico Tosi, Eleonora Ammannito, Filippo Giacomo Carrozzo, Maria Cristina De Sanctis, Andrea Raponi, Shane Byrne, Margaret E. Landis, Kynan H. G. Hughson, Carol A. Raymond, Christopher T. Russell

INTRODUCTION: Dwarf planet Ceres' low average-density (2162 ± 3 kg m^{-3}) indicates that it must contain considerable water. Water is likely a key component in the chemical evolution and internal activity of Ceres, possibly resulting in a layer of ice-rich material and perhaps liquid in the mantle. Mineral hydroxides (OH-bearing) and hydrates (H_2O-bearing), such as clays, carbonates, and various salts, would be created. These hypotheses were supported by the detection of hydroxyl (OH)–rich materials, OH-bearing molecule releases, H_2O vapor molecules, and haze. However, the presence of H_2O on the surface has not previously been confirmed. The detection and mapping of H_2O on Ceres is one objective of the Dawn spacecraft, in orbit around Ceres since March 2015.

ON OUR WEBSITE

Read the full article at http://dx.doi.org/10.1126/science.aaf3010

RATIONALE: The purpose of the Dawn space mission at Ceres is to study the geology, geophysics, and composition remotely by means of high-resolution imagery and spectrometry. Dawn's Visible and InfraRed Mapping Spectrometer (VIR) measures the sunlight scattered by the surface of Ceres in a range of wavelengths between 0.25 and 5.1 μm. The position and shape of absorption features in VIR reflectance spectra are sensitive to the surface mineral and molecular composition. In spectroscopy, absorption bands at 2.0, 1.65, and 1.28 μm are characteristic of vibration overtones in the H_2O molecule.

RESULTS: Dawn has detected water-rich surface materials in a 10-km-diameter crater named Oxo, which exhibit all absorption bands that are diagnostic of the H_2O molecule (see the figure). These spectra are most similar to those of H_2O ice, but they could also be attributable to hydrated minerals. Oxo crater appears to be geologically very young (~1 million to 10 million years); it has sharp rims and its floor is almost devoid of impacts, suggesting a recent exposure of surface H_2O. The high latitude and morphology of the Oxo crater protects much of the surface area from direct solar illumination for most of the cerean day, presenting favorable conditions for the stability of water ice or heavily hydrated salts.

CONCLUSION: Four ways to create or transport H_2O on Ceres are considered: (i) Exposure of near-surface H_2O-rich materials by a recent impact or an active landslide seems most consistent with the presence of both mineral hydrates and water ice. (ii) Release of subsurface H_2O may occur on Ceres, similar to release on comet nuclei, but may never recondense on the surface. (iii) Infall of ice-bearing objects is not likely to deposit water on Ceres, because the H_2O molecule likely would dissociate upon impact. (iv) Implantation of protons from the solar wind on the surface is not a probable origin of OH on Ceres because of the low flux of solar wind charged particles. We therefore conclude that surface H_2O or hydrated minerals are the most plausible explanation. ■

The list of author affiliations is available in the full article online.
*Corresponding author. Email: jean-philippe_combe@bearfightinstitute.com
Cite this article as J.-Ph. Combe *et al.*, *Science* **353**, aaf3010 (2016). DOI: 10.1126/science.aaf3010

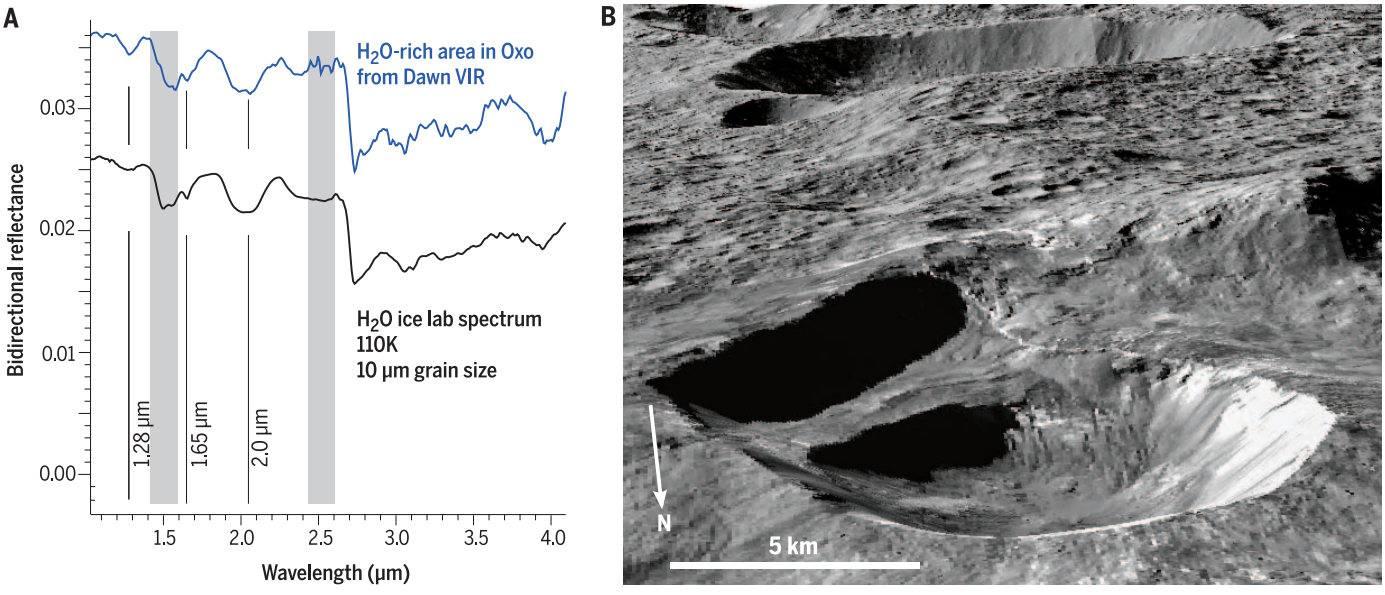

Dawn VIR infrared observations of Oxo crater on Ceres demonstrate the detection of H_2O at the surface. (**A**) Reflectance spectrum collected where absorption bands of H_2O at 1.28, 1.65, and 2 μm are the strongest (in blue) compared with a laboratory spectrum of H_2O ice (black). The lab spectrum is scaled and vertically shifted for clarity. (**B**) Perspective view of Oxo crater observed by the Dawn Framing Camera (FC), where the two high-albedo areas right next to the scarps contain H_2O-rich materials.

RESEARCH ARTICLE

PLANETARY SCIENCE

Detection of local H_2O exposed at the surface of Ceres

Jean-Philippe Combe,[1]* Thomas B. McCord,[1] Federico Tosi,[2] Eleonora Ammannito,[2,3] Filippo Giacomo Carrozzo,[2] Maria Cristina De Sanctis,[2] Andrea Raponi,[2] Shane Byrne,[5] Margaret E. Landis,[5] Kynan H. G. Hughson,[3] Carol A. Raymond,[4] Christopher T. Russell[3]

The surface of dwarf planet Ceres contains hydroxyl-rich materials. Theories predict a water ice-rich mantle, and water vapor emissions have been observed, yet no water (H_2O) has been previously identified. The Visible and InfraRed (VIR) mapping spectrometer onboard the Dawn spacecraft has now detected water absorption features within a low-illumination, highly reflective zone in Oxo, a 10-kilometer, geologically fresh crater, on five occasions over a period of 1 month. Candidate materials are H_2O ice and mineral hydrates. Exposed H_2O ice would become optically undetectable within tens of years under current Ceres temperatures; consequently, only a relatively recent exposure or formation of H_2O would explain Dawn's findings. Some mineral hydrates are stable on geological time scales, but their formation would imply extended contact with ice or liquid H_2O.

The state and abundance of water on the dwarf planet Ceres have been major questions ever since hydroxyl (OH)–rich materials were proposed as surface components (*1*, *2*) and eventually observed (*3*–*8*). The prediction of ice and perhaps liquid in the mantle (*9*–*11*), observations of sporadic releases of OH-bearing molecules (*12*), the detection of water vapor molecules (*13*), and reports of haze (*14*) support the presence of water on Ceres. Water is a key component in the chemical evolution and internal activity of planetary bodies, and products of aqueous activity such as bright carbonates have been observed on Ceres (*15*). Reflectance spectroscopy is sensitive to surficial water and hydroxyl groups; measurement of OH and H_2O absorptions near 1.5, 2.0, and 3 μm thereby allows for remote detection of H_2O. The depth of photon penetration depends on the material: Photons may penetrate a few micrometers into absorbing components such as those found on Ceres or other low-albedo surfaces, whereas they may penetrate several centimeters in highly scattering materials such as pure ice and snow (*16*).

Because Ceres has a low bulk density of 2162 ± 3 kg m^{-3} (*17*), its composition is expected to contain a substantial proportion of water. Internal heat (mostly from decay of radionuclides) is expected to have differentiated Ceres at least partially into a rocky core and icy mantle (*9*–*11*). Contact between silicates and ice or liquid water would have resulted in aqueous alteration of minerals, producing hydroxylated (OH-bearing) phases such as clays and carbonates (*5*–*7*, *9*–*11*, *15*), or mineral hydrates (H_2O-bearing) such as salts.

The Dawn mission at Ceres (*18*) is dedicated to the characterization of the geology, geophysics, and composition of this dwarf planet. The first observational orbit (Rotation Characterization) occurred on 23 April 2015 at an altitude of 13,500 km. The orbit was subsequently lowered to 4400 km for the Survey phase of the mission, which operated from 5 to 22 June 2015. The Dawn Visible and InfraRed (VIR) mapping spectrometer (*19*) senses surface composition by reflectance spectroscopy. It covers wavelengths of 0.25 to 5.1 μm with two detectors that measure radiance, overlap around 1 μm, and have spectral sampling of 1.9 nm and 9.8 nm for the visible and infrared, respectively. Initial global VIR analyses of Ceres identified the ubiquitous presence of phyllosilicates, but no H_2O-bearing species (*7*, *8*).

Here, we present VIR detections of H_2O-rich surface materials on Ceres from five observations of the crater Oxo, which is 10 km in diameter and is centered at 359.7°E, 42.2°N (*20*) (Fig. 1). The data were collected on 1 and 4 May 2015, with a spatial resolution of about 3.4 km per pixel, and on 6 and 9 June 2015, with a spatial resolution of about 1.1 km per pixel. Absorptions near 2 μm at the surface of Ceres require H_2O molecules, as they are attributable to an O-H stretch overtone in this molecule (*21*, *22*) commonly seen in spectra of water ice and mineral hydrates (*23*). Other O-H vibration overtones at 1.65 μm and 1.28 μm produce narrower yet meaningful absorption bands (*24*) that are visible in the VIR spectra. The three absorption bands at 1.28 μm, 1.65 μm (Fig. 2, D to F), and 2.0 μm (Fig. 2, G to I) occur within the same areas in the Oxo crater, which makes a strong case for the detection of H_2O. Similar to the rest of Ceres' surface, a strong and broad absorption around 3 μm due to the fundamental vibration mode of O-H is also observed. However, this spectral feature alone is not unique to H_2O, as only the OH group is required. Spectral models show that H_2O-ice spectra fit VIR observations better than any spectrum of mineral hydrates (Fig. 3); thus, we consider it the most likely surface component observed in the Oxo crater.

H_2O-rich materials are found within a high reflectance area on the pole-facing wall of the Oxo crater (Fig. 2) and possibly on the southeastern scarp above the rim. The crater is about 50% brighter at 1.1 μm than surrounding surface materials (Fig. 2, A and B). The surface on the H_2O-rich spot is characterized by temperatures 10 to 20 K lower than the rest of the crater (Fig. 2, J to L); this would be expected of exposed water ice (*25*), which has a higher thermal inertia than the average Ceres surface regolith, and of high-albedo materials in general.

Geological description of Oxo crater

In Fig. 1E, high-resolution images from the Framing Camera (FC) indicate that Oxo has sharp rims and few superposed craters, which implies that it is geologically young. It is also characterized by a scarp in the southeastern part. This terrace feature likely resulted from block collapse and slumping of the southeastern rim toward the center of the crater, forming a depression outside the crater. Long, arcuate fractures subparallel to the terrace scarp, well-defined talus material, and an extensive boulder field within Oxo indicate that the terrace block has been actively collapsing in the recent geologic past and may be continuing to do so at the present time. Several kilometer- and subkilometer-scale lobate flow features related to mass wasting have been observed on the northeastern and southeastern rims of the terrace block. These flows, particularly the examples observed near the H_2O-rich region, display several morphologic similarities (i.e., sharply defined flow margins, large rounded blunt snouts, and apparent mass concentration near the flow termini) to numerous other features on Ceres that have been interpreted as ice-cemented flows (*26*). The location of the strongest H_2O detection in Oxo exhibits a sloped hummocky texture that is divided in several locations by linear and sinuous gully-like depressions.

Calibration of spectra and spectral processing

Reflectance defines the ratio of irradiance from the surface of Ceres to the solar radiance flux. In this study, VIR spectra have been further corrected for the photometric effects of variable incidence and emergence angle due to the local topography. This correction is based on the Akimov disk-function model (*27*) and is similar to the processing of VIR data at Vesta performed for global mapping (*28*). We standardize bidirectional reflectances to incidence angles of 0° and emission angles of 30°.

The spectral slope measures the slope of a straight line fitted to VIR spectra between 1.0 and 2.4 μm. Maps of the spectral slopes were calculated

[1]Bear Fight Institute, 22 Fiddler's Road, P.O. Box 667, Winthrop, WA 98862, USA. [2]Istituto di Astrofisica e Planetologia Spaziali–Istituto Nazionale di Astrofisica, Rome, Italy. [3]Institute of Geophysics and Planetary Physics, University of California, Los Angeles, CA, USA. [4]Jet Propulsion Laboratory, Pasadena, CA, USA. [5]Lunar and Planetary Laboratory, Tucson, AZ, USA.
*Corresponding author. Email: jean-philippe_combe@bearfightinstitute.com

after normalization with respect to the local average reflectance between 1.0 and 2.4 μm for each pixel, and after division to the average spectrum of Ceres. The result is a spectral slope of zero for the average of Ceres.

The spectral feature centered at 1.5 μm in Fig. 1, E to G, might also be due to O-H vibration overtone; however, it must be interpreted cautiously because of light scattering between two order-sorting filters of the instrument (*8*), and thus it is not considered in this study. Although the diagnostic absorption feature of H_2O at 1.65 μm falls near one of these junctions, it is considered safe for interpretation. Several pieces of observational evidence indicate that instrument light scattering does not contribute significantly to the signal at this wavelength: (i) Light scattering creates spectral oscillations that stop around 1.6 μm, even for the strongest artifacts. (ii) The absorption band depths at 1.28 μm, 1.65 μm, and 2.0 μm have very similar distributions, consistent with the hypothesis that H_2O absorption is the main contributor of the 1.65-μm feature. (iii) The band depth parameter at 1.5 μm is mostly sensitive to albedo-contrasted surface features, which is radically different from the distribution pattern of absorptions attributed to H_2O.

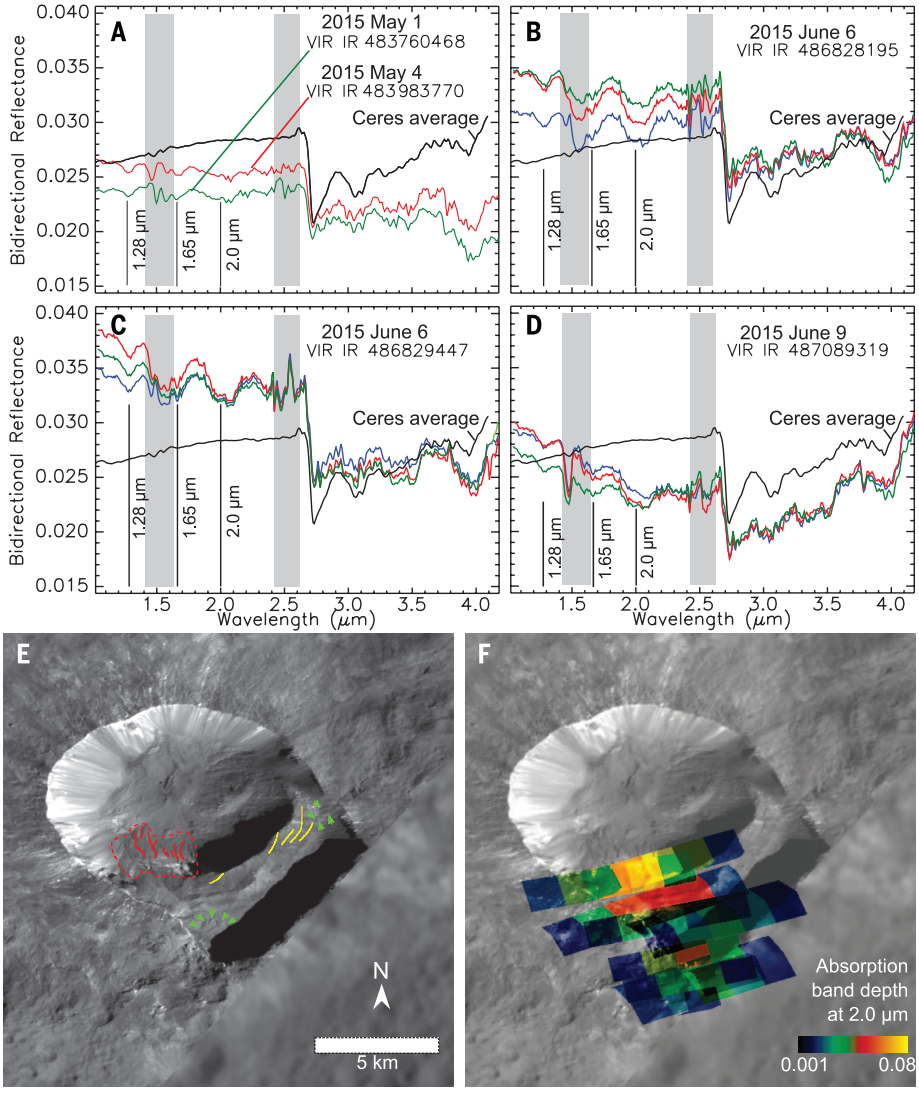

Fig. 1. Dawn VIR IR observations of Oxo crater on Ceres demonstrate the detection of H_2O at the surface. (**A** to **D**) Reflectance spectra collected where absorption bands of H_2O at 1.27, 1.65, and 2 μm are the strongest (in color) from distinct pixels within a VIR image. Each panel shows spectra from a different VIR image, except the average spectrum of Ceres (in black) displayed as a reference, showing no H_2O absorption bands. Gray rectangles define ranges of wavelengths where the spectra are the least reliable because they are at filter junctions [(*7*) and text]. (**E**) Oxo crater depicted by the Dawn Framing Camera in equirectangular projection. The red dashed line indicates the hummocky sloped material surrounding the region of strongest H_2O detection; solid red lines indicate linear and multiple juxtaposed (and partly overlapping) lobate mass wasting deposits. The yellow lines are superimposed upon arcuate fractures subparallel to the terrace scarp. The green arrows point toward the margins of lobate flow structures that are similar to other features on Ceres that have been interpreted as ice-cemented flows (*26*). (**F**) The same FC image mosaic as (A) is made brighter for clarity and overlain by the absorption band depth at 2 μm measured by the three VIR observations shown in (B) to (D). The area was more shaded during the acquisition of FC image than while VIR data were acquired.

Albedo and spectral characteristics of Oxo crater

Bright materials in the Oxo crater cover the northern and eastern rims, as well as a portion of the floor at the foot of the southern rim. The highly reflective unit has a negative spectral slope as a function of wavelength (bluer) in the near-infrared, whereas the rest of Ceres has a neutral or slightly positive spectral slope. VIR spectra with strong absorption bands at 1.28, 1.65, and 2 μm have a reflectance at 1.1 μm that is about 10% lower than the rest of the high-albedo unit and a moderately negative spectral slope (Fig. 2, M to O).

In Fig. 2F, VIR data from June 2015 overlain on FC images reveal that H_2O-rich materials correspond to high-albedo materials on the floor of the crater and possibly on the southeastern scarp above the rim. In all three observations, the illumination conditions (season and time of day) were similar, with a local incidence angle of 50° at noon local time. In an interval of 72.5 hours (nine cerean days), no variations of water absorption band depths could be measured, because instantaneous field of view of the observations did not overlap (Fig. 2F) and the H_2O-rich spot was likely smaller than a VIR pixel size (1.1 km). Only the two observations on 6 June 2015 sampled the high-albedo unit of the southern part of the crater floor, and both indicate an absorption band depth of about 8%. In the observation acquired on 9 June 2015, pixels were adjacent to only the bright spot—gaps exist between projected pixels because of the motion of the spacecraft—and the maximum absorption band depth measured was 3%.

Observations acquired in May 2015 (Fig. 1A) are consistent with an exposed H_2O-rich composition 1 month before the detection of the strongest absorption bands. The difference in spatial resolution between the Approach and Survey phases of the mission is sufficient to explain the differences in absorption band depth. These measurements suggest compositional stability within this time frame and a quantity of H_2O large enough to survive at the surface.

Spectral fitting by linear combination of spectra

Candidate materials (*9*, *11*) that exhibit absorption bands similar to VIR spectra of Oxo are free H_2O ice and H_2O-bearing minerals (mineral hydrates) such as chloride hydrates, magnesium sulfate hydrates ($MgSO_4$-nH_2O), ammonium sulfate hydrates (NH_4SO_4-nH_2O), sodium sulfate hydrates (Na_2SO_4-nH_2O), and sodium carbonate hydrates (Na_2CO_3-nH_2O), where n is the number of H_2O molecules per molecule of the mineral.

To interpret the composition of the H_2O-rich area in Oxo, we compared VIR spectra with laboratory spectra of several candidate materials by

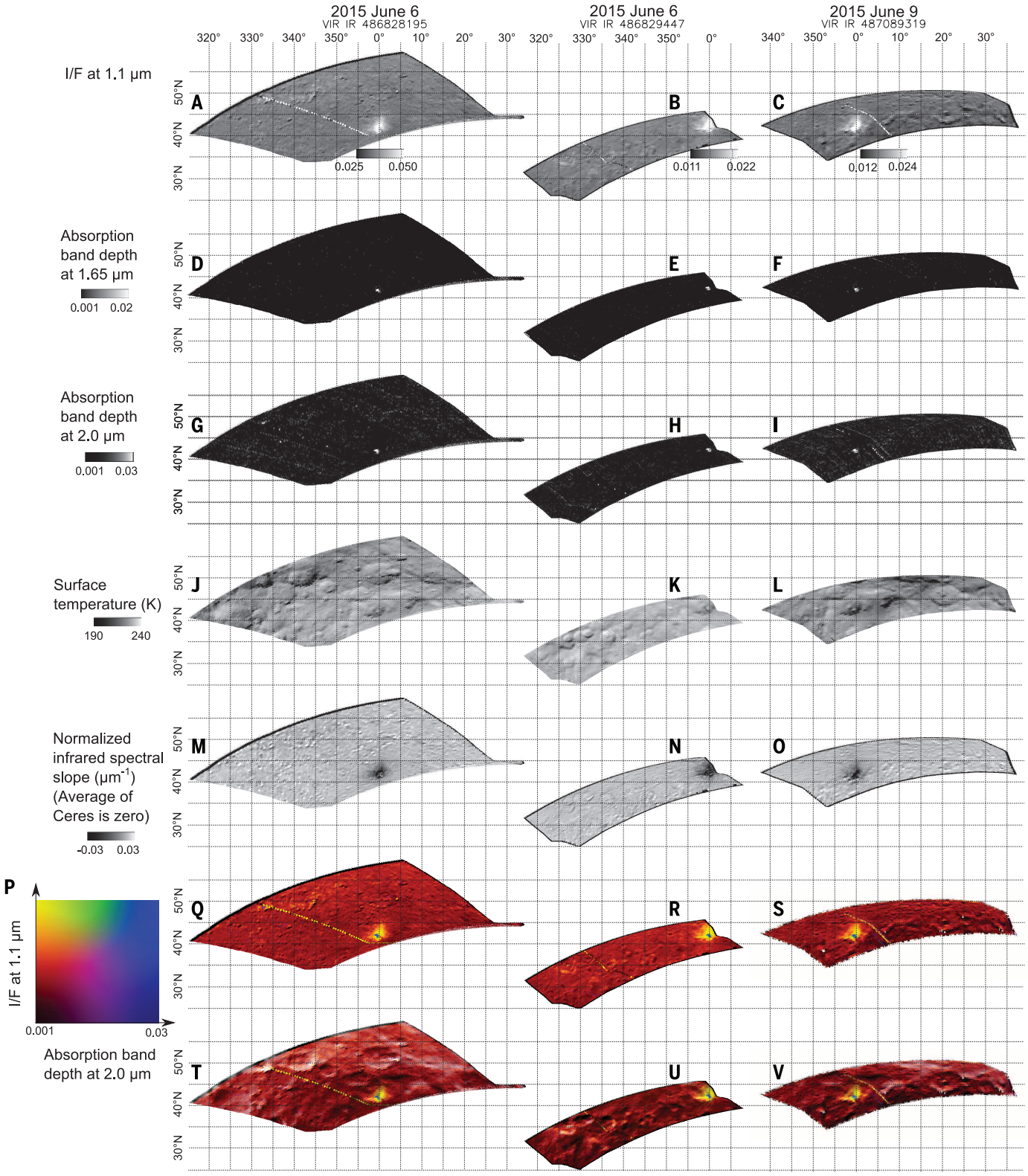

Fig. 2. Dawn VIR infrared observations of Oxo crater on Ceres obtained during the Survey phase of the mission demonstrate the detection of H_2O at the surface. (**A** to **C**) Reflectance at 1.1 μm, showing the location of a high-albedo surface unit. (**D** to **F**) Absorption band depth of H_2O at 1.65 μm. The brightest pixels correspond to the occurrence of the deepest absorption band. (**G** to **I**) Absorption band depth of H_2O at 2 μm. (**J** to **L**) Surface temperature retrieved from VIR data (*43*), which is also sensitive to terrain slopes. (**M** to **O**) Infrared spectral slope. (**P**) Two-dimensional color table that describes the meaning of the colors in (Q) to (V). (**Q** to **S**) Two spectral parameters (reflectance at 1.1 μm and absorption band depth at 2.0 μm) are represented in the same map, which illustrates the presence of H_2O-rich materials within the high-albedo unit. H_2O-rich materials (blue) exist within a high-albedo area (yellow) in the southern rim of the crater. (**T** to **V**) Same as (Q) to (S), except that the incidence angle with respect to the shape model of Ceres is overlain as a texture to better see the topography.

means of spectral modeling (29). An areal mixture is the simplest model, and it can be calculated by a linear combination of spectra. A linear spectral mixture does not necessarily represent light scattering in an ice-cemented regolith, which is an intimate mixture that results in nonlinear combinations of the spectra of each component. In addition, in the ranges of wavelengths of the H_2O absorption bands (where H_2O is mostly opaque), intimate mixing with a less absorbing material results in increased apparent overall reflectance and enhanced contrast of the absorption bands (23). This phenomenon of light scattering is also consistent with the fact that, in VIR spectra, the 2-μm absorption overtone of H_2O is almost as strong as the 3-μm fundamental absorption, which is never observed when H_2O ice is pure unless the 3-μm band is saturated. In Fig. 3 and Fig. 4, the spectra of pure components are multiplied by the coefficient of linear mixing; their sum added to the offset (dotted straight line) equals the modeled spectrum on top.

Figure 3 illustrates models (29) of spectral fitting of the same VIR spectrum with laboratory reflectance spectra of pure components between 1.02 and 2.5 μm at temperatures relevant to the asteroid belt and Jupiter satellites (30). Relative to VIR spectra, most chloride hydrates (31) have absorption bands of H_2O shifted toward shorter wavelengths (not represented here), except for frozen brines of the eutectic mixtures $MgCl_2$-12H_2O (Fig. 3F), KCl-H_2O, and NaCl-2H_2O. In all cases, laboratory spectra have a much higher reflectance than the surface of Ceres, which can be explained by mixtures on Ceres with low-albedo materials. The purpose of these comparisons is to visualize the position and shape of all the absorption bands associated with H_2O. Because the average spectrum of Ceres is relatively featureless between 1 and 2.5 μm (8), the models simulate these mixtures by scaling the reflectance spectra of pure components (gain) and by adding a spectrally neutral contribution (offset). The scaling factor is sensitive to the abundance of the H_2O-rich component, and the offset compensates empirically for some photometric effects and the absorption of neutral materials potentially present in the mixture. Achievement of a good quality of fit with this simple model indicates that several spectra of mineral hydrates can be considered in the interpretation and for future laboratory analyses, despite incomplete documentation of sample temperature and number of H_2O molecules in some mineral hydrates that are currently available.

Interpretation of linear combination of spectra

The spectral features of several H_2O-rich materials can fit VIR spectra for the small Oxo zone (Fig. 3). Among these candidates, H_2O ice provides the best fit of all (RMS = 0.00187%), hydrated sodium carbonates and hydrated magnesium sulfates are the next best (0.00262% < RMS < 0.00304%), and spectra of ammonium sulfates and sodium sulfates result in higher model residuals (RMS > 0.0032%). By definition, the RMS is proportional to the standard deviation of the residuals. For the best fit (Fig. 3A), the residuals from fitting an H_2O spectrum to the VIR spectrum of Oxo are on the same order of amplitude as the instrument calibration uncertainties, and their respective standard deviations are similar.

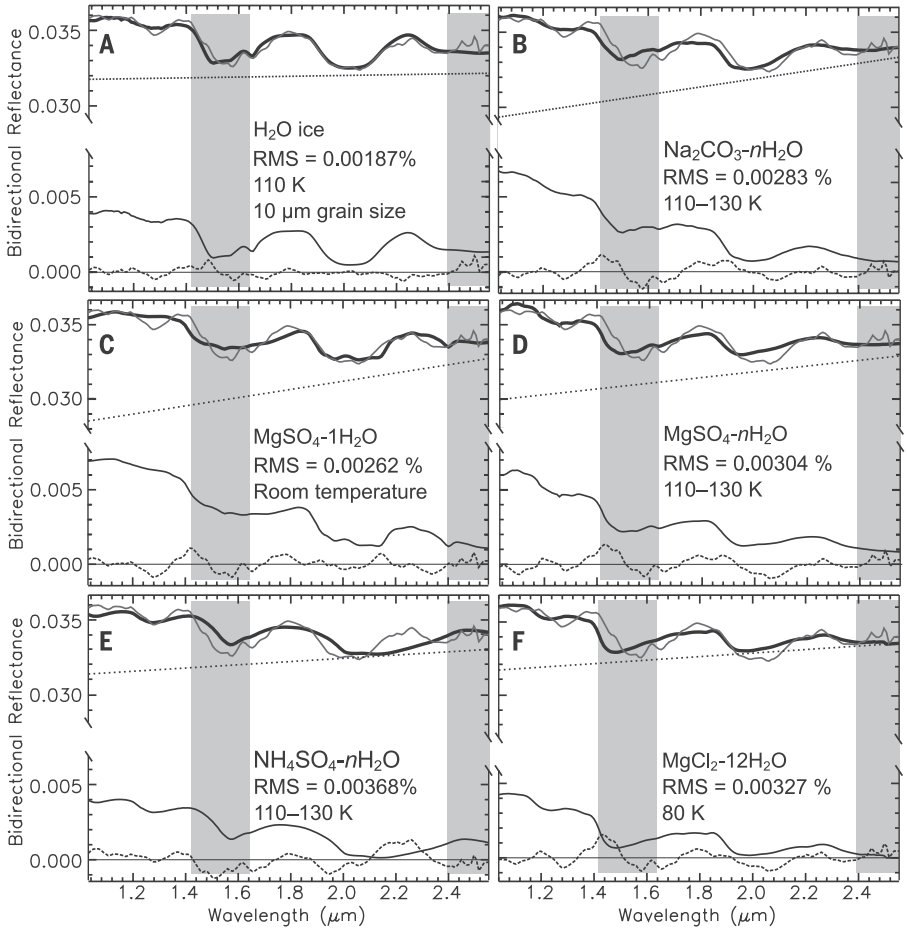

Fig. 3. Analysis and interpretation of the composition of H_2O-rich materials in Oxo. In each panel, one reflectance spectrum of the H_2O-rich zone in Oxo crater from Dawn VIR IR observation 486828195 (thin, black near top) is compared with a scaled reflectance spectrum of a pure hydrated component (thick, black). Gray rectangles define ranges of wavelengths where the spectra are the least reliable. Scaled laboratory spectra of several H_2O-rich samples (thin, black near bottom) and the offset (dotted line) used in each fit are shown. Near the bottom of each plot, model residuals (dashed curve) provide an indication of the quality of fit, along with the RMS value. (**A**) H_2O ice spectrum from the Johns Hopkins University Applied Physics Laboratory spectral library (22, 44). (**B**, **D**, and **E**) Spectra of mineral hydrates (30). (**C**) Monohydrated sulfate kieserite from the Reflectance Laboratory (RELAB) at Brown University (45). (**F**)The spectrum of frozen eutectic mixture $MgCl_2$-12H_2O is from (31).

Figure 4 presents the same VIR spectrum as in Fig. 1 from 1.02 to 4.2 μm, fitted with an H_2O ice spectrum linearly combined with the average spectrum of Ceres' surface and a spectral slope (straight line). The quality of fit over the extended range of wavelength, including the broad OH stretch fundamental absorption, demonstrates the presence of H_2O and confirms that water ice is the most likely component.

The scaling factor of 0.0057 in Fig. 4 only gives a lower limit for the proportion of H_2O ice in the surface covered by one pixel, because the H_2O-rich area in Oxo is not spatially resolved, and because low-albedo materials optically dominate when they are intimately mixed with a high-albedo material. Assuming, from Fig. 1, that the high-albedo area in Oxo crater floor is rich in H_2O ice, and that it corresponds to half of the surface covered by one pixel, then the proportion would be approximately 1% for the pixel that exhibits the strongest 2.0-μm absorption band. In the case of H_2O ice mixed with low-albedo material, over time, the sublimation of H_2O alone would leave a low-albedo lag deposit, forming a layer on top. Laboratory experiments of the effects of sprinkling charcoal grains on frost (22) indicate that reflectance decreases at a higher rate than the fractional areal coverage, and that a reflectance of 0.07 at 1 μm can be achieved with 30% areal coverage of ice. Our estimates from these calculations and assumptions is that the areal proportion of H_2O ice on the 1-km^2, high-albedo area is likely between 1 and 10%.

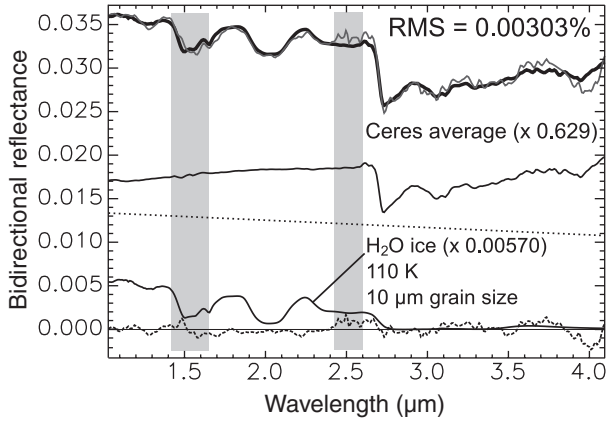

Fig. 4. Modeling of one reflectance spectrum of the H_2O-rich zone in the Oxo crater from Dawn VIR IR observation 486828195 with a linear combination (simulation of an areal mixture) of H_2O ice, the average spectrum of Ceres and a spectrally neutral, low-albedo spectral component (dotted straight line). This synthetic, spectrally neutral component also accounts for the relatively more negative spectral slope of the H_2O-rich area than the average spectrum of Ceres. The model residuals (dashed curve) and the RMS value document the quality of fit. Gray rectangles define ranges of wavelengths where the spectra are the least reliable.

Discussion

Among all VIR spectra acquired up to the Survey phase of the Dawn mission, Oxo is the only place on Ceres where we have found measurements of absorption band depth of 1% or more at 1.65 and 2.0 μm that correspond without ambiguity to the expected shape of H_2O absorption bands. These bands are most likely due to surface materials. Although cryovolcanic-like morphological features such as Ahuna Mons (*32*) suggest that H_2O ice might be present in the crust, hydrated salts were probably responsible for the liquid phase needed to form the mountain. However, H_2O-rich materials are not detected by spectroscopy at those places, because they are likely not exposed. There is no obvious connection with the finding of H_2O on the floor of the Oxo crater and previous reports of H_2O molecules above the surface of Ceres: (i) The location of Oxo differs from the reported H_2O molecule release on equatorial regions (*13*), and (ii) although haze was reported on Oxo and Occator (*14*), no surface H_2O has been identified by VIR within Occator (*15*).

The nature of the H_2O-rich surface of Oxo crater (H_2O ice or mineral hydrates) remains to be determined. VIR near-infrared spectra are better fitted by H_2O ice spectra than by hydrated minerals (Fig. 3); however, interpretation is still open. Thermodynamical properties can further constrain results provided by these initial observations. The small H_2O-rich area at Oxo may suggest a local origin. However, the finding of H_2O in a place that is likely protected from direct sunlight for most of the day (except around noon local time), even near summer solstice (solar longitude Ls was 81° on 6 to 9 June 2015), suggests the detected H_2O component could be more stable at this location because of limited direct solar illumination.

Pure surficial H_2O ice would sublime under current thermal conditions on Ceres (*25*, *33*, *34*), where daytime surface temperatures T span the range 180 to 240 K (*7*), with $T > 200$ K found in Oxo crater from 11 hours to 12 hours local solar time. This localized detection of exposed H_2O on the surface of Ceres could be consistent with predictions (*25*) of a near-surface ice table beginning at ~50° latitude, and of local surface ice deposits on a rough terrain; for example, at the latitude of Oxo, 1 m of pure, cohesive water ice would disappear within a few hundred years (*25*). Free water ice would require a relatively recent exposure of H_2O at the surface by landslides, by outgassing of water vapor followed by condensation, or by eruption of liquid water (cryovolcanism). According to some models, cometary-like activity or a landslide could expose H_2O ice mixed with dust. Depending on the amount of dust in the ice, it would become spectrally undetectable within 10 years (*33*, *35*) or tens of years because dust would become the dominant material within the optical thickness (a few micrometers at most). Even in the case of an ice-cemented regolith (more thermodynamically stable than pure water ice), the ablation rate would be significant over one cerean year.

We have estimated ice loss rates obtained by modeling surface and subsurface temperatures on Ceres by balancing surface insolation, thermal emission, and conduction to the subsurface (*33*) and incorporating a pole-vector determination from Dawn data. At 44°N, ablation is estimated to be 4 mm each cerean year, assuming horizontal ground, with an albedo of 13.5% and thermophysical parameters of ice-cemented regolith. At the solar longitude Ls = 81° when VIR observations were acquired, modeled water vapor production oscillated between 0.08 kg s^{-1} km^{-2} just before dawn to 0.22 kg s^{-1} km^{-2} in the afternoon. However, in the case of a pole-facing slope of 20°, ice loss is only ~50 μm of ice per cerean year, which makes the life span of a H_2O-ice rich layer about 80 times that of a flat surface.

Hydrated minerals could have formed very early in Ceres' evolution by contact with H_2O, either ice or liquid, before being exposed. Once at the surface, these species would dissociate at a slower rate than water ice, especially those with fewer H_2O molecule bonds (*30*, *36*). This is consistent with H_2O absorption bands of hydrated salts becoming asymmetric and shifted toward wavelengths shorter than 2 μm, sometimes by more than 0.1 μm, compared to water ice (Fig. 3), indicating higher energy and thus stronger bonds (*37*, *38*).

At least four ways to create or transport of H_2O on Ceres can be considered, listed here from the most likely to the least: (i) Exposure of endogenous near-surface H_2O-rich materials from an impact or local landslide could be consistent with both mineral hydrates and water ice. Other high-albedo units and young craters observed across Ceres may be preferential locations for searching for H_2O-rich materials. (ii) Release of subsurface H_2O occurs on comet nuclei and may exist on Ceres, although some models [e.g., (*35*)] predict that water vapor should not recondense. Long-lived radionuclide heat from the core (*9*–*11*) and potassium salts in the mantle or crust (*11*) may not be enough to drive endogenic activity that reaches the surface; however, collisions such as the one that created Oxo may have caused long-term activation (or reactivation) of regions with an ice-rich subsurface. (iii) Infall of hydrated meteorites or comets is a scenario that has brought OH-rich or H_2O-rich materials onto the surface of Vesta (*39*, *40*), and Oxo itself is a geologically recent impact (superposed crater counts suggest an age of less than 1 million to 10 million years); however, these H_2O molecules may well dissociate from the kinetic energy dissipated by the collision. (iv) The molecule of H_2O may form by implantation of protons from the solar wind as is the case on the Moon (*41*). Effects of the solar wind have not been observed on Vesta (*42*) despite a higher flux of solar wind particles [the distance from the Sun is shorter at Vesta (2.15 to 2.57 AU) than at Ceres (2.56 to 2.98 AU)]; therefore, this is not a probable origin of OH on Ceres.

REFERENCES AND NOTES

1. C. R. Chapman, J. W. Salisbury, Comparison of meteorite and asteroid spectral reflectivities. *Icarus* **19**, 507–522 (1973). doi: 10.1016/0019-1035(73)90078-X
2. T. B. McCord, M. J. Gaffey, Asteroids: Surface composition from reflection spectroscopy. *Science* **186**, 352–355 (1974). doi: 10.1126/science.186.4161.352; pmid: 17839866
3. L. A. Lebofsky, M. A. Feierberg, A. T. Tokunaga, H. P. Larson, J. R. Johnson, The 1.7- to 4.2-μm spectrum of asteroid 1 Ceres: Evidence for structural water in clay minerals. *Icarus* **48**, 453–459 (1981). doi: 10.1016/0019-1035(81)90055-5
4. P. Vernazza *et al*., Analysis of near-IR spectra of 1 Ceres and 4 Vesta, targets of the Dawn mission. *Astron. Astrophys.* **436**, 1113–1121 (2005). doi: 10.1051/0004-6361:20042506
5. A. S. Rivkin, E. L. Volquardsen, B. E. Clark, The surface composition of Ceres: Discovery of carbonates and iron-rich clays. *Icarus* **185**, 563–567 (2006). doi: 10.1016/j.icarus.2006.08.022
6. R. E. Milliken, A. S. Rivkin, Brucite and carbonate assemblages from altered olivine-rich materials on Ceres. *Nat. Geosci.* **2**, 258–261 (2009). doi: 10.1038/ngeo478
7. E. Ammannito *et al*., Distribution of phyllosilicates on Ceres. *Science* **353**, aaf4279 (2016).
8. M. C. De Sanctis *et al*., Ammoniated phyllosilicates with a likely outer Solar System origin on (1) Ceres. *Nature* **528**, 241–244 (2015). doi: 10.1038/nature16172; pmid: 26659184
9. T. B. McCord, C. Sotin, Ceres: Evolution and current state. *J. Geophys. Res.* **110**, E05009 (2005). doi: 10.1029/2004JE002244
10. P. C. Thomas *et al*., Differentiation of the asteroid Ceres as revealed by its shape. *Nature* **437**, 224–226 (2005). doi: 10.1038/nature03938; pmid: 16148926
11. J. Castillo-Rogez, T. B. McCord, Ceres' evolution and present state constrained by shape data. *Icarus* **205**, 443–459 (2010). doi: 10.1016/j.icarus.2009.04.008
12. M. F. A'Hearn, P. D. Feldman, Water vaporization on Ceres. *Icarus* **98**, 54–60 (1992). doi: 10.1016/0019-1035(92)90206-M
13. M. Küppers *et al*., Localized sources of water vapour on the dwarf planet (1) Ceres. *Nature* **505**, 525–527 (2014). doi: 10.1038/nature12918; pmid: 24451541

14. A. Nathues *et al*., Sublimation in bright spots on (1) Ceres. *Nature* **528**, 237–240 (2015). doi: 10.1038/nature15754; pmid: 26659183
15. M. C. De Sanctis *et al*., Bright carbonate deposits as evidence of aqueous alteration on (1) Ceres. *Nature* 10.1038/nature18290 (2016). doi: 10.1038/nature18290; pmid: 27362221
16. J. Dozier, R. O. Green, A. W. Nolin, T. H. Painter, Interpretation of snow properties from imaging spectrometry. *Remote Sens. Environ.* **113**, S25–S37 (2009). doi: 10.1016/j.rse.2007.07.029
17. C. T. Russell *et al*., Dawn arrives at Ceres: Exploration of a small, volatile-rich world. *Science* **353**, 1008 (2016).
18. C. T. Russell, C. A. Raymond, The Dawn mission to Vesta and Ceres. *Space Sci. Rev.* **163**, 3–23 (2011). doi: 10.1007/s11214-011-9836-2
19. M. C. De Sanctis *et al*., The VIR spectrometer. *Space Sci. Rev.* **163**, 329–369 (2011). doi: 10.1007/s11214-010-9668-5
20. Th. Roatsch *et al*., Ceres survey atlas derived from Dawn Framing Camera images. *Planet. Space Sci.* **121**, 115–120 (2016). doi: 10.1016/j.pss.2015.12.005
21. N. Ockman, thesis, University of Michigan (1957).
22. R. N. Clark, Water frost and ice: The near-infrared spectral reflectance 0.65-2.5 μm. *J. Geophys. Res.* **86**, 3087–3096 (1981). doi: 10.1029/JB086iB04p03087
23. R. N. Clark, P. G. Lucey, Spectral properties of ice-particulate mixtures and implications for remote sensing: I. Intimate mixtures. *J. Geophys. Res.* **89**, 6341–6348 (1984). doi: 10.1029/JB089iB07p06341
24. W. M. Grundy, B. Schmitt, The temperature-dependent near-infrared absorption spectrum of hexagonal H_2O ice. *J. Geophys. Res.* **103**, 25809–25822 (1998). doi: 10.1029/98JE00738
25. P. O. Hayne, O. Aharonson, Thermal stability of ice on Ceres with rough topography. *J. Geophys. Res.* **120**, 1567–1584 (2015). doi: 10.1002/2015JE004887
26. D. L. Buczkowski *et al*., The geomorphology of Ceres. *Science* **353**, aaf4332 (2016).
27. Yu. G. Shkuratov *et al*., Opposition effect from Clementine data and mechanisms of backscatter. *Icarus* **141**, 132–155 (1999). doi: 10.1006/icar.1999.6154
28. J.-Ph. Combe *et al*., Reflectance properties and hydrated material distribution on Vesta: Global investigation of variations and their relationship using improved calibration of Dawn VIR mapping spectrometer. *Icarus* **259**, 21–38 (2015). doi: 10.1016/j.icarus.2015.07.034
29. J.-Ph. Combe *et al*., Analysis of OMEGA/Mars Express data hyperspectral data using a Multiple-Endmember Linear Spectral Unmixing Model (MELSUM): Methodology and first results. *Planet. Space Sci.* **56**, 951–975 (2008). doi: 10.1016/j.pss.2007.12.007
30. T. B. McCord, G. Teeter, G. B. Hansen, M. T. Sieger, T. M. Orlando, Brines exposed to Europa surface conditions. *J. Geophys. Res.* **107**, 5004 (2002). doi: 10.1029/2000JE001453
31. J. Hanley, J. B. Dalton III, V. F. Chevrier, C. S. Jamieson, R. S. Barrows, Reflectance spectra of hydrated chlorine salts: The effect of temperature with implications for Europa. *J. Geophys. Res.* **119**, 2370–2377 (2014). doi: 10.1002/2013JE004565
32. O. Ruesch *et al*., Geologically recent cryo-volcanic activity on Ceres. *Science* **353**, aaf4286 (2016).
33. F. P. Fanale, J. R. Salvail, The water regime of asteroid (1) Ceres. *Icarus* **82**, 97–110 (1989). doi: 10.1016/0019-1035(89)90026-2
34. T. Titus, Ceres: Predictions for near-surface water ice stability and implications for plume generating processes. *Geophys. Res. Lett.* **42**, 2130–2136 (2015). doi: 10.1002/2015GL063240
35. M. Formisano, M. C. De Sanctis, G. Magni, C. Federico, M. T. Capria, Ceres water regime: Surface temperature, water sublimation and transient exo(atmo)sphere. *Mon. Not. R. Astron. Soc.* **455**, 1892–1904 (2016). doi: 10.1093/mnras/stv2344
36. M. Y. Zolotov, E. L. Shock, Composition and stability of salts on the surface of Europa and their oceanic origin. *J. Geophys. Res.* **106**, 32815–32827 (2001). doi: 10.1029/2000JE001413
37. A. Novak, Hydrogen bonding in solids, correlation of spectroscopic and crystallographic data. *Struct. Bonding* **18**, 177–212 (1974). doi: 10.1007/BFb0116438
38. T. B. McCord *et al*., Hydrated salt minerals on Europa's surface from the Galileo near-infrared mapping spectrometer (NIMS) investigation. *J. Geophys. Res.* **104**, 11827 (1999). doi: 10.1029/1999JE900005
39. M. C. De Sanctis *et al*., Detection of widespread hydrated materials on Vesta by the VIR Imaging Spectrometer on board the Dawn mission. *Astrophys. J.* **758**, L36 (2012). doi: 10.1088/2041-8205/758/2/L36
40. T. B. McCord *et al*., Dark material on Vesta from the infall of carbonaceous volatile-rich material. *Nature* **491**, 83–86 (2012). doi: 10.1038/nature11561; pmid: 23128228
41. T. B. McCord *et al*., Sources and physical processes responsible for OH/H_2O in the lunar soil as revealed by the Moon Mineralogy Mapper (M^3). *J. Geophys. Res.* **116**, E00G05 (2011). doi: 10.1029/2010JE003711
42. C. M. Pieters *et al*., Distinctive space weathering on Vesta from regolith mixing processes. *Nature* **491**, 79–82 (2012). doi: 10.1038/nature11534; pmid: 23128227
43. F. Tosi *et al*., Thermal measurements of dark and bright surface features on Vesta as derived from Dawn/VIR. *Icarus* **240**, 36–57 (2014). doi: 10.1016/j.icarus.2014.03.017
44. J. W. Salisbury, D. M. D'Aria, A. J. Wald, Measurements of thermal infrared spectral reflectance of frost, snow, and ice. *J. Geophys. Res.* **99**, 24235–24240 (1994). doi: 10.1029/94JB00579
45. J. F. Mustard, C. M. Pieters, Photometric phase functions of common geologic minerals and applications to quantitative analysis of mineral mixture reflectance spectra. *J. Geophys. Res.* **94**, 13619–13634 (1989). doi: 10.1029/JB094iB10p13619

ACKNOWLEDGMENTS

Support for this research was provided under the NASA Dawn mission through subcontract 2090-S-MB516 from the University of California, Los Angeles. The VIR instrument and VIR team are funded by ASI (Italian Space Agency) and INAF (Istituto Nazionale di Astrofisica). The involvement of S.B. and M.E.L. was made possible by award NNX15AI29G of the Dawn Guest Investigator Program. Dawn data for Ceres are archived in NASA's Planetary Data System Small Bodies Node (http://sbn.pds.nasa.gov/data_sb/target_asteroids.shtml#1_Ceres). We thank J. Castillo-Rogez, B. Ehlmann, H. Y. McSween, C. M. Pieters, P. Schenk, S. Schröder, and S. Uy for valuable discussions and critical reading of the manuscript.

5 February 2016; accepted 22 June 2016
10.1126/science.aaf3010